Sign Reversal of Magnetoresistance and Inverse Spin Hall effect in

Doped Conducting Polymers

Dali Sun^{1,2*}, Yaxin Zhai², Kipp J. van Schooten², Chuang Zhang^{2,3}, Marzieh Kavand², Hans

Malissa², Matthew Groesbeck², Reghu Menon⁴, Christoph Boehme², and Z. Valy Vardeny²

¹Department of Physics, North Carolina State University, Raleigh, North Carolina 27695, USA

²Department of Physics and Astronomy, University of Utah, Salt Lake City, Utah 84112, USA

³ Institute of Chemistry, Chinese Academy of Sciences, Beijing, 100019 China

⁴Department of Physics, Indian Institute of Science, Bangalore 560012, India

Abstract. Conducting polymers, where pristine polymers are doped by active dopants, have been

used in a variety of flexible optoelectronic device applications due to their tunable conductivity

values. Charge transport in these materials has been intensively studied for over three decades.

However, spin transport properties in these compounds have remained elusive. Here, we studied

two polaron-dominated and trap-dominated spin transport processes in two types of PEDOT:PSS

polymers that are lightly and heavily doped, respectively. Using pulsed spin-pumping and spin-

injection techniques, we found the sign of inverse spin Hall effect and magnetoresistance

obtained from the lightly doped PEDOT:PSS film can reverse its polarity as a function of

temperature and applied bias, in contrast to that in the heavily doped PEDOT:PSS film. Our

work provides an alternative approach for studying the spin transport in conducting polymer

films.

Keywords: Conducting polymers, spin pumping, inverse spin Hall effect, magnetoresistance

*Corresponding Author, E-mail: dsun4@ncsu.edu

1

Introduction

Poly(3,4-ethylenedioxythiophene) (PEDOT) doped with polystyrene sulfonate (PSS), PEDOT:PSS, has been widely employed in various organic-based optoelectronic devices owing to its excellent tunable conductivity value, long-term stability, thin-film processability, and reproducibility¹⁻⁶. Remarkably, the conductivity of PEDOT:PSS can be tuned from 10⁻⁵ to 10³ S/cm depending on the solvent, additive, and processing method used⁷⁻⁹. The major charge carriers in most of PEDOT:PSS conducting polymers are considered to be either localized or weakly delocalized polarons that usually undergo hopping process⁵. However, recently bipolaron-dominated charge transport in doped PEDOT with Tosylate (PEDOT:Tos)¹⁰ or triuoromethanesulfonate (OTf) anion (PEDOT:OTf)¹¹ has attracted intensive interest. These doped PEDOT compounds exhibit very high conductivity, semi-metallic behavior, and a large Seebeck coefficient with applications in thermoelectric devices.

PEDOT:PSS has also been investigated as a promising spin-mediating compound for spintronics applications, where spin-aligned carriers play a key role in transmitting, processing, and storing information. However, the fabrications of PEDOT:PSS-based spin valves have been challenging and not demonstrated so far^{12,13}. Alternatively, PEDOT:PSS has been reported as a solution-processed organic spin-charge converter¹⁴, although the spin-to-charge conversion efficiency has been found to be small due to the weak spin-orbit coupling (SOC) in this material. Beyond the challenges of devices fabrication and performance, the most puzzling part is the spin transport mechanism through conducting polymers. Polarons were proposed to dominate spin diffusion in poly[2,5-bis(3-tetradecylthiophen-2-yr)thieno[3,2-b]thiophene] (PBTTT)¹⁵, whereas other mechanisms have been suggested as well. For instance, it has been proposed that spin diffusion

is dominated by impurities¹⁶⁻¹⁸. Hence, in order to elucidate the spin transport mechanism in the organic compounds particularly conducting polymers, the ability to distinguish between polaron-dominated and trap- or impurity-dominated spin diffusion is essential.

Here we report two methods to study the spin transport in the PEDOT:PSS films. Our proposed approaches may be used to distinguish between the observations of polaron-dominated and trapor impurity-dominated spin transport that have been debated for years. Two types of PEDOT:PSS films were investigated: A low conductivity PEDOT:PSS (Al4083 with σ~10⁻³ S/cm) and a high conductivity PEDOT:PSS (PH1000 with $\sigma \sim 300$ S/cm). Using the recently developed pulsed spin-pumping method^{19,20}, we were able to observe subtle spin-to-charge conversions in these two types of PEDOT:PSS films, characterized by a pulsed inverse spin Hall (ISHE) response. We found that the pulsed ISHE response reverses polarity in the low conductivity PEDOT:PSS film at low temperature compared with that at room temperature, while the polarity of ISHE response in the high conductivity PEDOT:PSS film remains unchanged between two temperatures. The polarity change also occurs in the magnetoresistance (MR) response of spin-valves based on the low conductivity PEDOT:PSS compound: A positive MR response is obtained in the Ohmic regime of the I-V curve at low bias, whereas a negative MR response occurs at high bias in the trap-filling regime. The sign reversal is attributed to two different spin diffusion mechanisms dominated by polaron diffusion and impurity-mediated spin transport, respectively, caused by different doping concentrations in two compounds. Our work may present a new way of studying polaron- and trap-based spin transport in conducting polymers utilizing their distinct spin-dependent responses.

I-V response characteristics of the PEDOT:PSS films

Two types of PEDOT:PSS compounds were selected in this study (both are CleviosTM PEDOT:PSS purchased from Heraeus). In the 'Al4083' compound, the ratio of PEDOT to PSS is 1:6. Because of this small ratio, Al4083 is a relatively poor conductor (in-plane conductivity $\sigma \parallel \sim 10^{-3}$ s/cm, out-of-plane conductivity $\sigma \perp \sim 10^{-8}$ s/cm) that is widely used as a hole transport layer in organic light-emitting diodes and organic photovoltaic cells. The other type of PEDOT:PSS material is 'PH1000', in which the ratio of PEDOT to PSS is 1:2.5. The higher concentration of PSS dramatically increases the conductivity of this type of PEDOT:PSS, which may reach to 10^3 S/cm depending on the percentage of the dopant molecules. PH1000 has been used as an alternative to the metal-based electrode in various applications that require flexible organic optoelectronic devices²¹. We note that approximately one charge carrier is doped per three ethylene-dioxythiophen units²², from which we could estimate the carrier concentration of $\sim 1 \times 10^{20}$ cm⁻³ and $\sim 3 \times 10^{20}$ cm⁻³ in Al4083 and PH1000, respectively.

In-plane and out-of-plane I-V measurements were performed in both PEDOT:PSS films as a function of temperature (see Figure 1). For the in-plane I-V measurement, PEDOT:PSS solutions were spin-cast (at 3000 rpm) on top of SiO₂/Si substrates, on which two Al stripes (200 nm thick, 200 µm × 4 mm) with a gap of 1 mm were grown by electron-beam evaporation. The spin-coated films were annealed at 110°C in a glove box with an inert nitrogen atmosphere. For the out-of-plane I-V measurements, the PEDOT:PSS solution was spin-coated on top of 1 mm wide ITO etched stripes, followed by the same annealing procedure. The substrate area surrounding the ITO strip was covered by a 200 nm thick SiO₂ in order to prevent the formation of short circuits during the fabrication process. The as-prepared PEDOT:PSS devices were subsequently

transferred into a deposition chamber in which Au top electrodes were thermally evaporated in a cross-bar configuration. The I-V responses were measured using a Keithley 2400 source-meter in a closed-loop cryostat under vacuum.

Figure 1(a) and (b) show the typical I-V characteristics of Al4083 and PH1000 PEDOT:PSS film along the in-plane direction at room temperature, respectively. The in-plane conductivity of the PH1000 device, σ_{\parallel} is several orders of magnitude higher than that of Al4083, which is consistent with literature reports⁴. While the in-plane conductivity in PH1000 is relatively high, its out-of-plane conductivity, σ_{\perp} , is, as expected⁴, much lower ($\sigma_{\perp} \sim 10^{-4}$) as shown in Figure 1(d). Similarly, σ_{\perp} in Al4083 ($\sigma_{\perp} \sim 10^{-8}$, Figure 1(e)) is several orders of magnitude lower than its σ_{\parallel} .

The temperature dependence of conductivity for both types of PEDOT:PSS films are shown in Figure 1(c). The applied voltage was kept low (V = 1.0V for PEDOT:PSS (PH), V = 50V for PEDOT:PSS (Al)) in order to study the I-V characteristics of both PEDOT:PSS films in the Ohmic regime. The conductance in PH1000 shows a very weak temperature dependence. This suggests that the high concentration of delocalized polarons dominates the diffusive-type carrier transport in this heavily doped PH1000 film. In contrast, the conductance of the Al4083 film changes by about two orders of magnitude between room temperature and low temperature, indicating a typical hopping transport. Furthermore, at the lowest temperature, the I-V response in the Al4083-based device exhibits a linear Ohmic response at a low bias voltage (V < 0.5V, see Figure 3b), but changes to a strong nonlinear response at high bias (V > 0.5V). This nonlinear response is routinely observed in organic semiconductor-based devices and has been ascribed to a trap-filling regime, in which impurity states become filled with the injected carriers before a

space-charge-limited current sets in²³. This also suggests that the charge transport in the Ohmic regime is dominated by traps, in contrast to the delocalized polaron transport within the heavily doped PH1000 film. At room temperature, thermally activated hopping of carrier generation overcomes the energy barrier of shallow traps, which leads to conductivity enhancement in the Al4083 film. A summary of the obtained electrical parameters of the two PEDOT films is given in Table 1.

Spin pumping and inverse spin Hall effect measurements

We have studied the inverse spin Hall effect (ISHE) that results from the spin current in the organic layer generated via spin pumping from the FM substrate in both types of PEDOT:PSS film¹⁹. As shown in Figure 2(a), during the spin-pumping process the microwave (MW) absorption by the FM film in the presence of an external magnetic field, B, induces precession of the magnetization, M(t), in the FM layer, which, in turn, excites magnons. At the FM/organic interface, the magnon excitations undergo back-scattering into the FM substrate, and thus their angular momentum is transferred to the electron-polarons in the organic material. This process aligns the spin-½ polarons along the magnetic field direction, inducing a pure spin current, J_S , without the impedance mismatch problem observed in other types of spin-pumping²⁴. The spin current is then detected using the ISHE, in which the spin current J_S carrying spin polarization σ induces an electric field E_{ISHE} given by the relation $E_{ISHE} \propto \theta_{ISHE} J_S \times \sigma^{25}$. Therefore, the induced E_{ISHE} is perpendicular to both, spin and spin current, as shown in Figure 2(a). In this relation, θ_{ISHE} is defined as the spin Hall angle, which describes the efficiency of the spin-to-charge conversion process, namely conversion from the injected spin current into charge

current²⁵. Recent studies have found that n-type and p-type doped GaAs semiconductors show ISHE response with opposite sign²⁴. It is noteworthy that the polarity of charges in electrons and holes cannot be simply accounted for the reversed sign of ISHE response in GaAs films: the spin polarization direction is the same for both types of spin-aligned carriers that are determined by the same magnetization of ferromagnetic over-layer. The same direction of transverse electric field created by ISHE moves the holes to one end while moving electrons to the other end, thus generating the same polarity of electric voltage. The opposite sign of ISHE is attributed to the opposite sign of spin Hall angle for the majority carriers in n-type and p-type GaAs film, depending on their distinct intrinsic SOC. We therefore conclude that the ISHE measurements of PEDOT:PSS films may be a powerful tool to investigate the spin-aligned carriers in these compounds¹⁹.

Recently we have developed a pulsed spin pumping technique that outperforms the continuous wave (CW) method in terms of detecting subtle spin-currents, particularly in the weak spin-orbit coupling regime, as in the class of organic molecules and polymers such as PEDOT:PSS^{19,20}. In the pulsed-ISHE experiment, the device has a FM/organic two-layer structure connected by two small metal electrodes with a 50 µm gap underneath the device area [see Figure 2(a)]. We use Ni₈₀Fe₂₀ (NiFe) as the FM layer for spin pumping into the adjacent nonmagnetic organic layer. Cu electrodes were used because of the negligible SOC of Cu, which does not interfere with the ISHE process in the organic layer. In order to substantially reduce the anisotropic magnetoresistance (AMR), planar Hall effect (PHE), anomalous Hall effect (AHE), and other spurious effects in the p-ISHE measurements, especially for organic-based samples with a very weak spin-orbit coupling, we integrated a microwave shunt capacitor layer (SiO₂) into the device

geometry¹⁹. The microwave shunt capacitor effectively absorbs the electric field component of microwave in the cavity and suppresses the AHE and other artefacts. In addition the shunt capacitor suppresses the ISHE response from Cu electrode, as well as possible AMR and PHE contributions from the NiFe layer. Other thermal-related artefact sources (e.g. resonant heating, and its resulting spin-Seebeck effect, anomalous Nernst effect, etc.) are very much suppressed under application of ns- to μs-duration pulsed FMR excitation having very low duty cycle (<0.25%)¹⁹.

The low conductivity PEDOT:PSS (Al4083, $\sigma \parallel \sim 10^{-3}$ S/cm) was initially studied due to its good processability and surface flatness. An all-metallic NiFe/Pt bilayer device with the identical structure served as a reference sample. The devices were placed at the center of a low-Q cavity with MW pulse excitation (5 µs duration) at 9.63 GHz and 500 Hz repetition rate (Bruker pulsed EPR spectrometer^{19,20}). The peak pulsed MW power was ~ 1 kW, which results in an amplitude of the magnetic component of the MW field, B_1 , of 1.1 mT at the sample location. The in-plane external static magnetic field B was applied along the film plane [see Figure 2(a) for the definition of θ_H]. The pulsed ISHE response was detected by the induced electromotive force, V_{ISHE} using a Femto DHPCA 100 current amplifier for metals, and a Stanford Research SRS 570 current amplifier with bandwidth set at 100Hz-1MHz for organic polymers. The current amplifier output was connected to the input of a Bruker SpecJet transient recorder (250 MS/s, 8-bit digitizer) that is built into the ElexSys spectrometer. The sensitivity of the current amplifier was 10^{-3} A/V (Femto DHPCA-100) or 20μ A/V (SRS 570). The pulsed ISHE(B) response measurements were averaged over 10240 repetitions.

A typical broadband ferromagnetic resonance (FMR) response of a NiFe/PEDOT:PSS (Al4083) device, acquired with a home-built coplanar waveguide structure, is shown in Fig. 2(b). In the inset, the width of the measured FMR band is shown as a function of the MW frequency, from which the Gilbert damping factor, α , is derived using linear fitting²⁵. Compared to the intrinsic α_0 obtained from a pure NiFe single layer, the enhancement of the damping factor ($\Delta\alpha=\alpha-\alpha_0$) in NiFe/PEDOT:PSS device suggests that additional dissipation occurs due to the magnons at the NiFe/PEDOT:PSS interface. This damping is due to the generation of a pure spin current (J_S) in the PEDOT:PSS film¹⁹. These results are consistent with the haracteristic of spin pumping via the MW excitation, indicating the efficient spin-pumping at the NiFe/PEDOT:PSS (Al4083) interface.

Next, we focus on the polarity of the pulsed ISHE voltage response in order to identify the type of spin-aligned carriers in the two PEDOT:PSS films. Figure 2(c) shows the field dependence of the $V_{\rm p-ISHE}$ at a MW pulse power of $P=1{\rm kW}$ measured at $\theta_{\rm H}=0^{\circ}$ (B) and $\theta_{\rm H}=180^{\circ}$ (-B) for the NiFe/PEDOT:PSS (Al4083) device at room temperature. The maximum $V_{\rm p-ISHE}$ occurs at the FMR resonance field, $B_{\rm res}$, and shows a negative sign at $\theta_{\rm H}=0^{\circ}$ and positive a sign at $\theta_{\rm H}=180^{\circ}$, which is in agreement with the results obtained for the NiFe/Pt reference device [see Figure 2(c) inset]. This indicates that the spin-aligned charge carriers in PEDOT:PSS (Al4083) have the same sign of spin Hall angle as the Pt device.

The pulsed ISHE response of the same NiFe/PEDOT:PSS(Al4083) device was measured also at T=3.5K. In addition to the reduced ISHE amplitude at this low temperature, we found a polarity change of the observed ISHE response as compared to the response at T=300K, namely a

positive ISHE at $\theta_{\rm H}=0^{\circ}$ but negative at $\theta_{\rm H}=180^{\circ}$. We note that the obtained asymmetry of the ISHE response at the two measured angles originates from a heating effect (via the Seebeck effect or other artifacts, which universally exhibit negative induced voltage at *both* orientations) at low temperature when the device is irradiated with MW. Similarly, low temperature pulsed ISHE measurements were also performed on the NiFe/Pt reference sample. In contrast to the PEDOT:PSS device, the ISHE polarity in the reference device remains unchanged at low temperature.

The intrinsic SOC determines the sign of the spin Hall angle and consequently the polarity of ISHE response. Nevertheless, it is thus not possible to have a polarity change at low temperature for one specific type of carrier, even due to a drastic change of intrinsic SOC. The change of charge polarity between the electrons and holes cannot explain the reversed ISHE response and there is only one type of carriers in both PEDOT:PSS films (i.e., holes). The MW induced heating effect can be ruled out in the pulsed measurement and would remain the same polarity for the same device which is in contrast to our observations. Therefore the reverse ISHE polarity of the NiFe/PEDOT:PSS (Al4083) device suggests that there are another type of charge carrier that is responsible for the spin transport at T=3.5K, in which the *effective SOC* has an opposite polarity. We conclude that there are two types of charge carriers in the PEDOT:PSS(Al) film. One carrier type dominates spin transport at room temperature, and the other carrier type governs spin transport at low temperature. Each charge carrier type possesses an opposite spin Hall angle polarity, producing the reversal of the ISHE response at two temperatures.

In order to scrutinize our conclusions, we measured the pulsed ISHE in a NiFe/PEDOT:PSS(PH) bilayer device at T=300K (Figure 2(e)) and T=3.5K (Figure 2(f)), respectively. From the I-V characteristic versus temperature of the PH1000 film, we established that the conductivity exhibits only a very weak temperature dependence in this PEDOT:PSS formulation. This suggests that, for this control device, there is only one type of carrier (i.e. delocalized polarons) that is responsible for spin transport throughout the entire temperature range. In this case, the ISHE polarity in the NiFe/PEDOT:PSS(PH) should remain the same at 300 K and 3.5 K. Indeed, we found the same ISHE polarity at these two temperatures, as shown in Figures 2(e) and 2(f), which supports our assumption.

Electrically spin injection and magnetoresistance measurements

While spin-pumping measurements provide direct evidence for the two types of spin transport through the observed polarity reversal at low temperature, the change of shallow trap occupation and polaron spin transport in the PEDOT:PSS (Al4083) is achieved *passively* by varying the temperature. In principle, the shallow traps can be filled by electrically injected spin-aligned carriers from the metal electrode, as obtained in the I-V response at low temperature [see Figure 3(b)].

To achieve comparable changes in shallow trap occupancy with carrier injection, we fabricated a PEDOT:PSS-based vertical organic spin-valve (OSV) devices²⁷ and studied the magnetoresistance (MR) to *actively* control the spin transport from the two types of injected spin currents that may occur in the different injection regimes, namely the Ohmic regime and trap-

filling regime. For the OSV devices, we used a typical FM1/PEDOT:PSS/FM2 structure, as depicted in Figure 3(a). In this structure, the PEDOT:PSS device is placed between the two FM electrodes with different coercive fields. The top electrode (FM1) is made out of cobalt, a hard FM material (10 nm) with a coercive field, B_{c1} (Co)~120 mT and a spin polarization degree $(c\sim30\%)$ that is nearly independent of temperature²⁷. An Al layer (100 nm) was deposited on top of the Co layer to prevent oxidation. The half-metal La_{0.67}Sr_{0.33}MnO₃ (LSMO) was used for the bottom FM electrode (FM2) since it is an air-stable soft FM material $[B_{c2} \text{ (LSMO)} \approx 5 \text{ mT}]$ with Curie transition temperature $T_c = 307$ K and a high spin polarization degree ($P_2 \sim 98\%$) at cryogenic temperatures²⁷. The MR of the fabricated devices was measured in a closed-cycle refrigerator at 11 K under a positive voltage on the LSMO electrode, while varying an external in-plane magnetic field, **B** [see Figure 3(a)]. The four-point resistance, R, of the OSV strongly depends on the relative magnetization orientation of the two FM electrodes, named R_P and R_{AP} for the respective parallel and anti-parallel magnetization configurations. The figure-of-merit of a spin-valve is defined by its maximum MR value within the MR(B) response, which is given by the relation $MR_{max} = (R_{AP} - R_P)/R_P$.

Figure 3(b) shows a typical I-V characteristic of the PEDOT:PSS (Al4803) based OSV device at 11K. The I-V response contains two regimes: an Ohmic regime ($I \propto V$) with constant resistance at low bias voltage, and a trap-filling (TFL) regime ($I \propto V^r$) caused by the injected charge carriers that fill the existing traps in the organic film²². The MR response was measured for both regimes at the same temperature.

As shown in Figures. 3(c) and 3(d), a clear MR response is observed in both regimes. Since the coercive field of Co (~120 mT) is much larger than that of the LSMO (~5 mT) at 11K, the relative magnetization orientation in the two FM electrodes are anti-parallel to each other when the external field B is between B_{c1} and B_{c2} . In contrast, the magnetizations are oriented parallel to each other when the field strength $B > B_{c2}$ [see the insets in Figure 3(c)]. The resistance of the anti-parallel alignment is higher than that of the parallel alignment in the Ohmic regime with $V = \pm 0.5$ V. Remarkably, we found that the MR polarity at both V = +0.8 V (Figure 3(e)) and V = -0.8 V (Figure (3f)) are reversed compared to that within $V = \pm 0.5$ V. The coercive fields of two FM electrodes at different bias voltages remain unchanged. The slightly shifted coercive field at the low and high voltage bias is caused by a non-hysteretic high field magnetoresistance background from the LSMO electrode²⁷.

A reversed MR polarity was reported in an Alq₃-based organic spin valve where a ferroelectric layer of PbZr_{0.2}Ti_{0.8}O₃ (PZT) is inserted between the Alq₃ layer and LSMO electrode²⁸. However, a similarly reversed MR response should not be anticipated here in the absence of the ferroelectric layer. We also note that the reversed MR response emerges at a relatively low voltage bias, indicating that the modified barrier due to the high voltage bias between LSMO and PEDOT:PSS is unlikely accounted for this effect^{29,30}. Tunneling anisotropic magnetoresistance (TAMR), which has been demonstrated to occur in the LSMO-based spin valves cannot explain the reversal in MR response either since the TAMR polarity does not change with the bias voltage³¹.

We thus concluded that the MR polarity change at high bias voltage originates from the injection of charge carriers from FM electrode into the PEDOT:PSS layer in the trap-filling regime. In our devices, the work functions of LSMO, PEDOT:PSS, and Co are 4.9 eV, 5.2 eV, and 4.8 eV, respectively, and thus LSMO is considered to be the hole injector^{27,28}. At lower bias in the Ohmic regime, only a small number of injected holes is trapped. The spin transport in this regime is dominated by these 'trap-limited' carriers that have a low mobility and conductivity, exhibiting a positive MR response. As the bias increases, more injected carriers fill the shallow traps and thus nearly-free carriers that require less hopping energy may dominate the charge transport, similar to the delocalized polaron transport in the PEDOT:PSS (PH1000) film. Therefore, the MR is negative similar to that of the MR response in the Alq₃-based OSV devices. The reversal of MR polarity of the PEDOT:PSS (Al4083) device is therefore consistent with the results from spin-pumping and ISHE measurements.

4. Conclusion

In summary, by combining pulsed ISHE and MR measurements at different temperatures, we distinguish between delocalized polaron and trap-dominated spin transport in lightly doped PEDOT:PSS film (Al4083) from their distinctive ISHE and MR responses. Specifically, the negative ISHE response and the positive MR value correspond to the trap-dominated spin transport, where the Al4083 film is at low temperature and small bias. When polarons dominate the spin transport, the Al4083 film exhibits a negative MR value and a positive ISHE response, which is similar to the behavior of heavily doped PEDOT:PSS (PH1000). Our work provides a new avenue to study the mechanism of spin transport in organic semiconductors.

Acknowledgments

Y.Z., K.J.v.S., and C.Z. were supported by the Utah NSF–Material Science & Engineering Center (Grant No. DMR-1121252). M.G., M.K., and H.M. were supported by NSF grant No. DMR-1701427. D.S. was supported by the start-up grant from North Carolina State University.

Reference:

- 1. C. K. Chiang, C. R. Fincher, Jr., Y. W. Park, A. J. Heeger, H. Shirakawa, E. J. Louis, S. C. Gau and A. G. MacDiarmid, "Electrical Conductivity in Doped Polyacetylene". *Phys. Rev. Lett.* **39**, 1098 (1977).
- 2. S. R. Forrest, "The path to ubiquitous and low-cost organic electronic appliances on plastic". *Nature* **428**, 911-918 (2004).
- 3. P. K. H. Ho, D. S. Thomas, R. H. Friend, and N. Tessler, "All-Polymer Optoelectronic Devices". *Science* **9**, 233-236 (1999).
- 4. C. S. S. Sangeeth, M. Jaiswal and R. Menon, "Correlation of morphology and charge transport in poly(3,4-ethylenedioxythiophene)—polystyrenesulfonic acid (PEDOT–PSS) films". *J. Phys: Cond. Matt.*, **21**, 072101 (2009).
- 5. Y. Chen, Y. Zhao and Z. Liang, "Solution processed organic thermoelectrics: towards flexible thermoelectric modules". *Energy Environ. Sci.*, **8**, 401-422 (2015).
- 6. A. Elschner, S. Kirchmeyer, W. Lövenich, U. Merker and K. Reuter, *PEDOT: Principles and Applications of an Intrinsically Conductive Polymer* (CRC press, Taylor and Francis Group, LLC) (2011).
- 7. N. Massonnet, A. Carella, O. Jaudouin, P. Rannou, G. Laval, C. Cellea and J.-P. Simonato, "Improvement of the Seebeck coefficient of PEDOT:PSS by chemical reduction combined with a novel method for its transfer using free-standing thin films". *J. Mater. Chem.* C 2, 1278-1283 (2014).
- 8. S. Liu, H. Deng, Y. Zhao, S. Ren and Q. Fu, "The optimization of thermoelectric properties in a PEDOT:PSS thin film through post-treatment". *RSC Adv.*, **5**, 1910-1917 (2015).

- 9. A. J. Kronemeijer, E. H. Huisman, I. Katsouras, P. A. van Hal, T. C. T. Geuns, P. W. M. Blom, S. J. van der Molen and D. M. de Leeuw, "Universal Scaling in Highly Doped Conducting Polymer Films". *Phys. Rev. Lett.* **105**, 156604 (2010).
- O. Bubnova, Z. U. Khan, H. Wang, S. Braun, D. R. Evans, M. Fabretto, P. Hojati-Talemi,
 D. Dagnelund, J.-B. Arlin, Y. H. Geerts, S. Desbief, D. W. Breiby, J. W. Andreasen, R.
 Lazzaroni, W. M. Chen, I. Zozoulenko, M. Fahlman, P. J. Murphy, M. Berggren and X. Crispin,
 "Semi-metallic polymers". *Nature Materials* 13, 190-194 (2014).
- 11. N. Massonnet, A. Carella, A. de Geyer, J. Faure-Vincentc and J.-P. Simonato, "Metallic behaviour of acid doped highly conductive polymers". *Chem. Sci.*, **6**, 412-417 (2015).
- 12. T. V A G de Oliveira1, M. Gobbi1, J. M Porro1, L. E Hueso and A. M Bittner, "Charge and spin transport in PEDOT:PSS nanoscale lateral devices". *Nanotechnology* **24**, 475201 (2013).
- 13. Y. Kawasugi, M. Ara, H. Ushirokita, T. Kamiya and H. Tada, "Preparation of lateral spin-valve structure using doped conducting polymer poly(3,4-ethylenedioxythiophene) poly(styrenesulfonate)". *Organic Electronics* **14**, 1869-1873 (2013).
- 14. K. Ando, S. Watanabe, S. Mooser, E. Saitoh and H. Sirringhaus, "Solution-processed organic spin-charge converter". *Nature Materials* **12**, 622-627 (2013).
- 15. S. Watanabe, K. Ando, K. Kang, S. Mooser, Y. Vaynzof, H. Kurebayashi, E. Saitoh & H. Sirringhaus, "Polaron spin current transport in organic semiconductors". *Nature Physics* **10**, 308–313 (2014).
- 16. Z. G. Yu. "Suppression of the Hanle Effect in Organic Spintronic Devices". *Phys. Rev. Lett.* **111**, 016601 (2013).

- 17. Z. G. Yu. "Impurity-band transport in organic spin valves". *Nature Communications* **5**, 4842 (2014).
- 18. S. W. Jiang, S. Liu, P. Wang, Z. Z. Luan, X. D. Tao, H. F. Ding, and D. Wu. "Exchange-Dominated Pure Spin Current Transport in Alq₃ Molecules". *Phys. Rev. Lett.* **115**, 086601 (2015).
- 19. D. Sun, K. J. van Schooten, M. Kavand, H. Malissa, C. Zhang, M. Groesbeck, C. Boehme & Z. Valy Vardeny. "Inverse spin Hall effect from pulsed spin current in organic semiconductors with tunable spin–orbit coupling". *Nature Materials* **15**, 863–869 (2016).
- 20. M. Kavand, C. Zhang, D. Sun, H. Malissa, Z. V. Vardeny, and C. Boehme. "Quantitative inverse spin Hall effect detection via precise control of the driving-field amplitude". *Phys. Rev. B* **95**, 161406(R) (2017).
- 21. Yong Hyun Kim, Christoph Sachse, Michael L. Machala, Christian May, Lars Müller-Meskamp, and Karl Leo. "Highly Conductive PEDOT:PSS Electrode with Optimized Solvent and Thermal Post-Treatment for ITO-Free Organic Solar Cells". *Adv. Funct. Mater.* 21, 1076-1081 (2011).
- 22. S. Kirchmeyer et al, PEDOT:principles and applications of an intrinsically conductive polymer.(CRC Press, Taylor & Francis Group, 2011)
- 23. M. Pope and C. E. Swenberg, *Electronic Process in Organic Crystals and Polymers*, Oxford University Press, Oxford, 2nd edn (1999).
- 24. K. Ando, S. Takahashi, J. Ieda, H. Kurebayashi, T. Trypiniotis, C. H. W. Barnes, S. Maekawa and E. Saitoh, "Electrically tunable spin injector free from the impedance mismatch problem". *Nature Materials* **10**, 655-659 (2011).

- 25. K. Ando, S. Takahashi, J. Ieda, Y. Kajiwara1, H. Nakayama1, T. Yoshino, K. Harii1, Y. Fujikawa, M. Matsuo, S. Maekawa and E. Saitoh, "Inverse spin-Hall effect induced by spin pumping in metallic system". *J. Appl. Phys.* **109**, 103913 (2011).
- 26. <u>L. Chen, S. Ikeda, F. Matsukura, and H. Ohno, "DC voltages in Py and Py/Pt under ferromagnetic resonance"</u>. *Applied Physics Express* **7**, 013002 (2014).
- 27. Z. H. Xiong, D. Wu, Z. V. Vardeny and J. Shi, "Giant magnetoresistance in organic spin-valves". *Nature*, **427**, 821-824 (2004).
- 28. D. Sun, M. Fang, X. Xu, L. Jiang, H. Guo, Y. Wang, W. Yang, L. Yin, P. C. Snijders, T. Z. Ward, Z. Gai, X.-G. Zhang, H. N. Lee & J. Shen, "Active control of magnetoresistance of organic spin valves using ferroelectricity". *Nature Communications*, **5**, 4396 (2014).
- 29. S. W. Jiang, B. B. Chen, P. Wang, Y. Zhou, Y. J. Shi, F. J. Yue, H. F. Ding, and D. Wu. "Voltage polarity manipulation of the magnetoresistance sign in organic spin valve devices". *Appl. Phys. Lett.* **104**, 262402 (2014).
- 30. K.-R. Jeon, B.-C. Min, I.-J. Shin, C.-Y. Park, H.-S. Lee, Y.-H. Jo, and S.-C. Shin, "Electrical spin accumulation with improved bias voltage dependence in a crystalline CoFe/MgO/Si system". *Applied Physics Letters* **98**, 262102 (2011).
- 31. M. Grünewald, M. Wahler, F. Schumann, M. Michelfeit, C. Gould, R. Schmidt, F. Würthner, G. Schmidt, and L. W. Molenkamp. "Tunneling anisotropic magnetoresistance in organic spin valves". *Phys. Rev. B* **84**, 125208 (2011).

Figure Captions

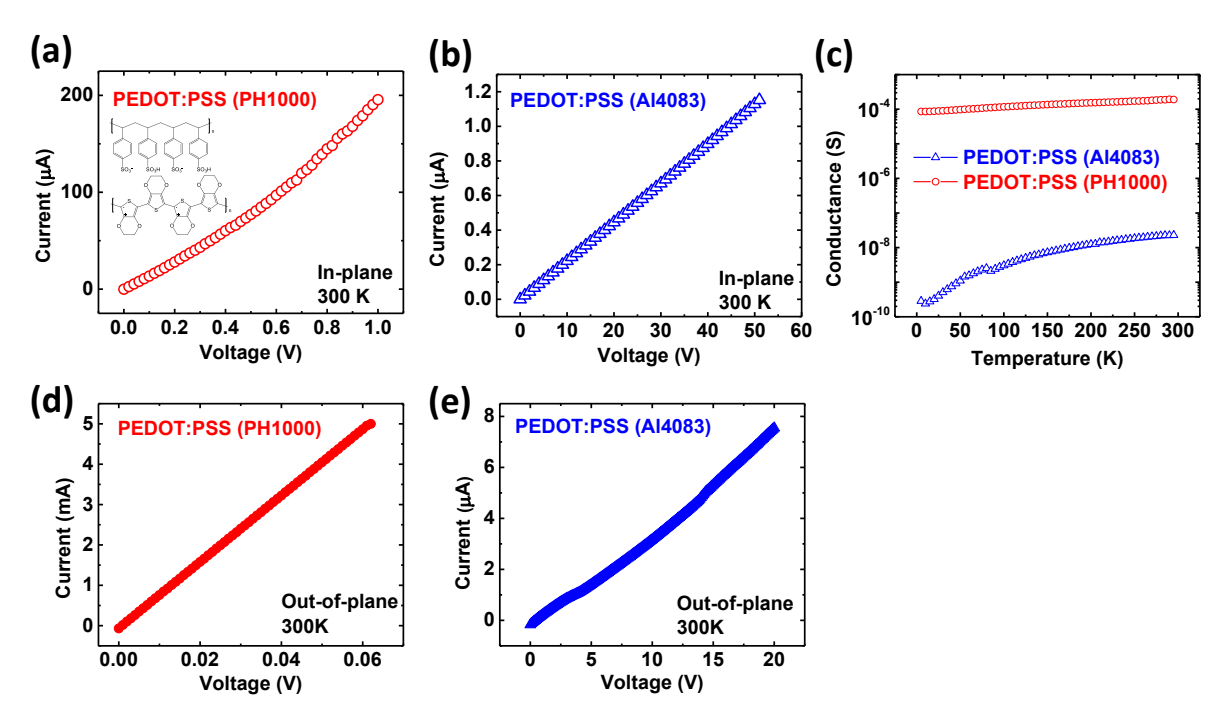


FIG.1 (a) and (b) Room temperature in-plane I-V characteristics in two types of doped PEDOT:PSS spin-coated films, namely lightly doped PEDOT:PSS (Al4083) and heavily doped PEDOT:PSS (PH1000), respectively. The inset shows the schematic molecular structure of doped PEDOT:PSS. (c) Measured in-plane conductance (σ||) as a function of temperature for the two PEDOT:PSS films. (d) and (e) out-of-plane I-V characteristics in spin-coated PH1000 and Al4083 film, respectively.

Table 1. A summary table for the obtained electrical transport properties of two PEDOT:PSS films investigated. σ , μ , and n presents the conductivity, mobility, and carrier concertation along the parallel (||) and out-of-plane (\perp) direction, respectively.

PEDOT:PSS	PEDOT:PSS ratio	σ ()	μ ()	σ (⊥)	μ (⊥)	n
		(s/cm)	(cm ² /Vs)	(s/cm)	(cm ² /Vs)	(cm ⁻³)
A14083	1:6	0.0068	4× 10 ⁻⁴	4× 10 ⁻⁸	2× 10 ⁻⁹	$\sim 1 \times 10^{20}$
PH1000	1:2.5 with 1% DMSO	268	6	8× 10 ⁻⁵	2× 10 ⁻⁶	$\sim 3 \times 10^{20}$

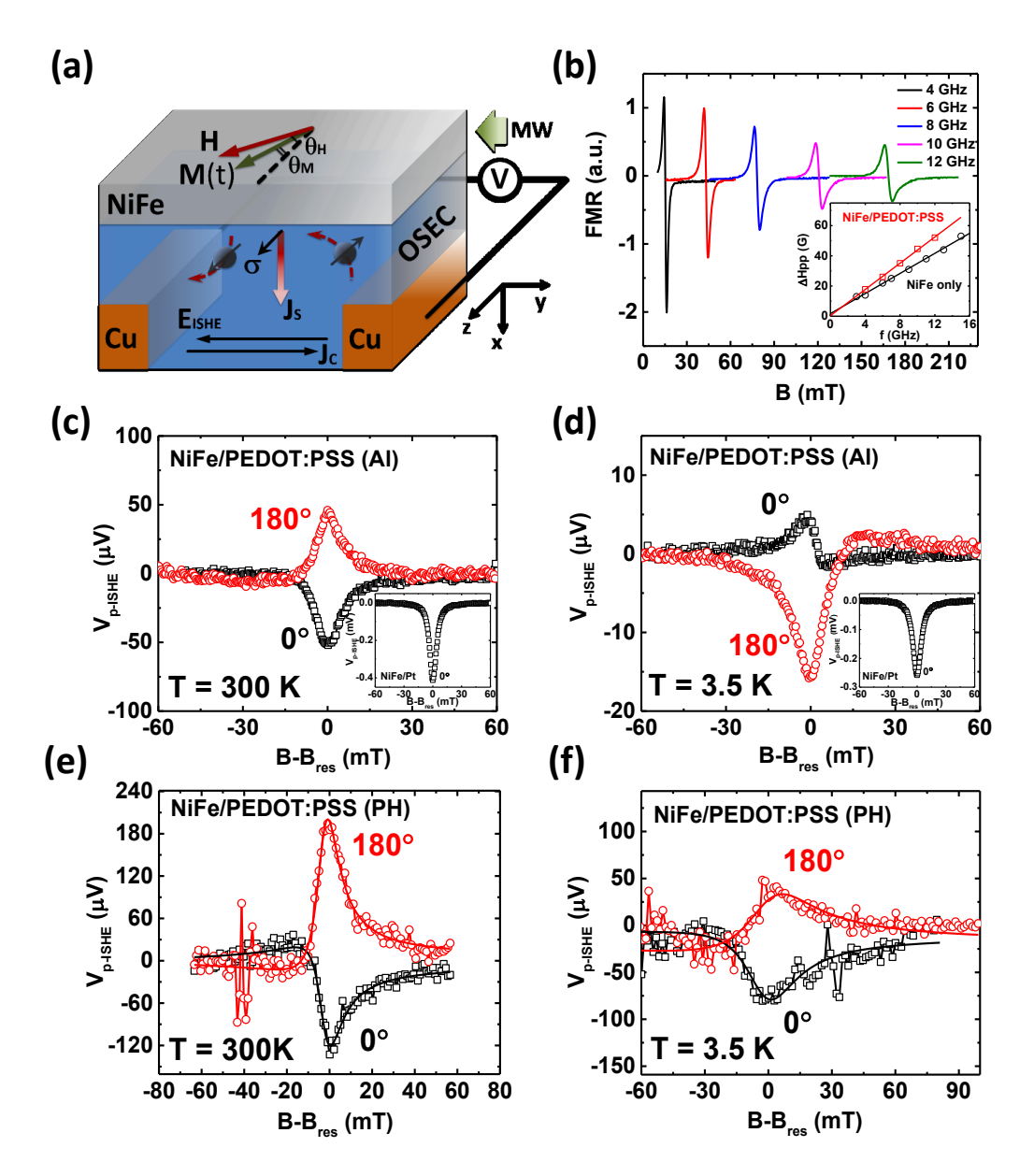


FIG. 2 (a) Schematic of the spin-pumping process and the set up for measuring the ISHE current. (b) Field dependence of the broadband FMR spectrum of the NiFe/PEDOT:PSS (Al4083) device at $\theta_H = 0^\circ$. The inset shows the width of FMR band in bare NiFe and NiFe/PEDOT:PSS bilayer as a function of the microwave frequency, from which the damping factor, α , can be derived. (c) and (d), The field dependence of V_{p-ISHE} in NiFe/PEDOT:PSS (Al4083) device at 300 K and 3.5K, respectively. The black squares and red circles data were measured at in-plane magnetic field, $B = (\theta_H = 0^\circ)$ and $-B = (\theta_H = 180^\circ)$, respectively. Reproduced from Ref. 19, Supp. Information, with permission of Nature Publishing Group. The insets show the V_{p-ISHE} response of the a NiFe/Pt device measured under the same conditions. (e) and (f) Field dependence of V_{p-ISHE} in NiFe/PEDOT:PSS (PH) device at 300K and 3.5K, respectively.

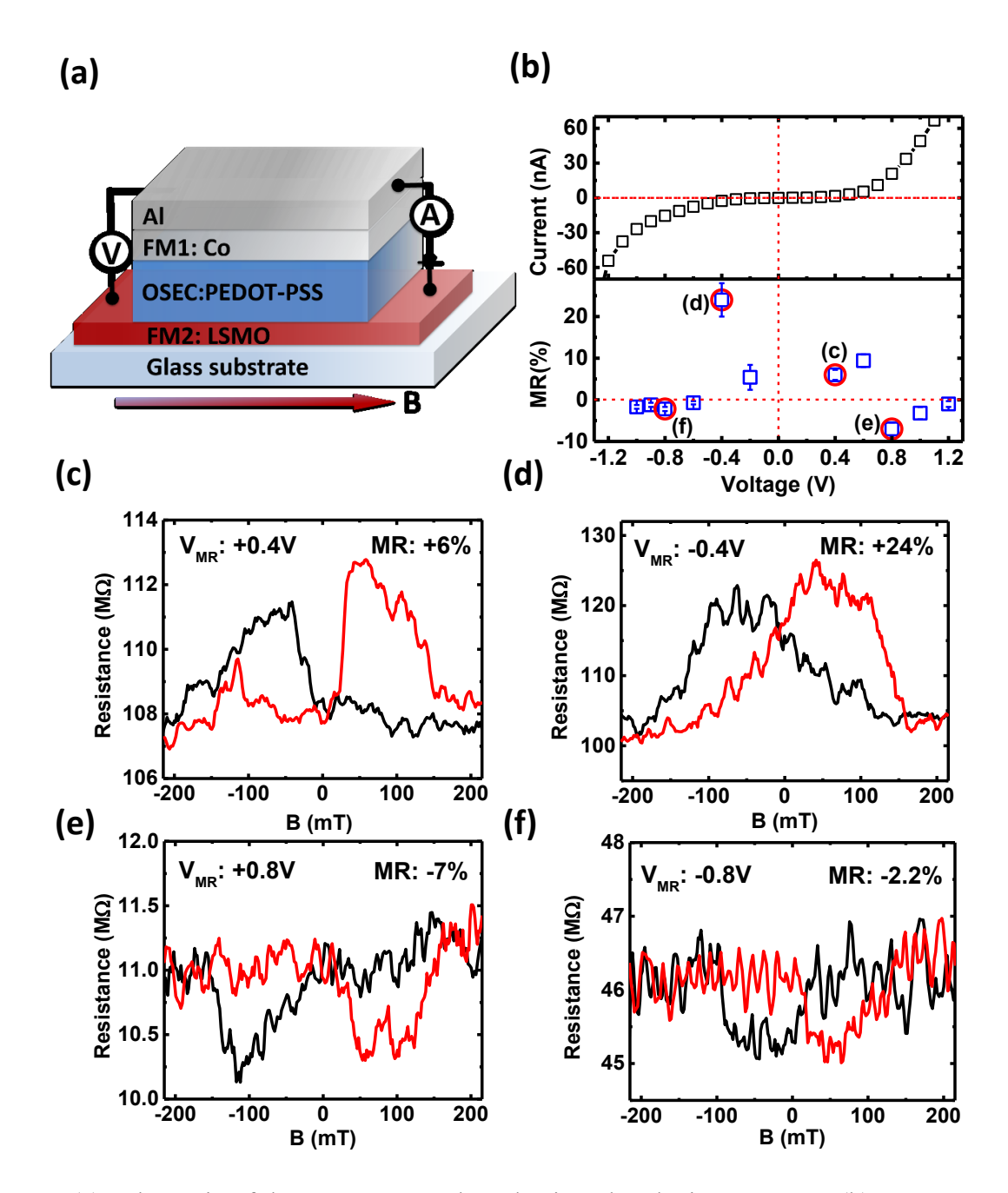


FIG. 3 (a) Schematic of the PEDOT-PSS-based spin valve device structure. (b) Upper panel: the typical I-V characteristics of the PEDOT:PSS (Al4083)-based OSV at 5K. Bottom panel: the MR value at various applied bias voltages. (c)-(f) MR(B) responses of PEDOT:PSS (Al4083) OSV device at four bias voltages measured at 5K (c) +0.4V, (d) -0.4V, (e) +0.8V and (f) -0.8V. The black (red) curve denotes MR(B) response measured upon decreasing (increasing) B. The respective anti-parallel (AP) and parallel (P) configurations of the FM magnetization orientations are shown in the insets. The MR response in PEDOT:PSS OSV reverses its sign between the low (Ohmic regime) and high (trap-filling regime) bias voltage.